Progress In Electromagnetics Research, Vol. 156, 135–144, 2016

Satellite Multibeam Coverage of Earth: Innovative Solutions and Optimal Synthesis of Aperture Fields

Andrea F. Morabito[1, 3, *], Antonia R. Laganà[1, 3], and Loreto Di Donato[2, 3]

Abstract—The problem of the synthesis of optimal continuous aperture sources to optimally realize the satellite multibeam coverage of Earth is stated and solved. The design approach relies on a far-field representation which exploits at best the degrees of freedom arising from the geometrical structure of the well-known four-colors coverage map. The overall synthesis is stated as a Convex Programming problem wherein the fast achievement of the (unique) globally optimal solution is guaranteed. The introduced tools allow stating the ultimate theoretical radiation performances achievable by any circular-aperture antenna of fixed size and, at the same time, can be exploited as a reference in the synthesis of isophoric direct-radiating arrays. Numerical examples concerning a mission scenario recently proposed by the European Space Agency are provided.

1. INTRODUCTION

The demand of satellite communications involving higher and higher data rates, e.g., Broadband Internet Access and TV services such as High-Definition Television (HDTV) and Three-Dimensional Television (3DTV), is continuing to grow [1–6]. This trend has a large impact on the electromagnetic specifications of the communication links. Moreover, the demand of high data rates lives together with one of small user antennas which require satellite high values of both the Equivalent Isotropically Radiated Power (EIRP) and the ratio between the antenna gain and noise temperature (G/T). This circumstance, combined with the necessity to cover large Earth regions as well as with the fact that the antenna directivity is inversely proportional to the area of its beam footprint, pushes towards the utilization of *multibeam* antennas [1–6].

A well-known and effective multibeam coverage scheme is shown in Fig. 1, which has been devised by the European Space Agency (ESA) to provide services from Geostationary Earth Orbit (GEO) satellites [4]. In this canonical mission scenario, the region to be covered is hexagonally sampled into a number of circular spots having the same size and a constant center-to-center spacing. Each beam has been assigned a specific frequency sub-band and a specific polarization in order to avoid interferences amongst adjacent spots [4]. In particular, two different sub-bands (i.e., two portions of the Ku and Ka bands, respectively) and two different polarizations (i.e., the left-hand and right-hand circular polarizations) are adopted, so that four non-interfering beams are realized. The interfering spots, i.e., the 'iso-frequency' and 'iso-polarization' regions, are indicated by the same color, leading to the well-known 'four-colors' map (see Fig. 1). The extreme effectiveness of this coverage scheme is guaranteed by the well-known Four Colors Theorem, which establishes that "any map in a plane can be colored using four colors in such a way that regions sharing a common boundary (other than a single point) do not share the same color" [7]. In particular, while three is the minimum number of different channels which can be used in any reuse scheme [5, 6], four is a very common choice [8–11].

Received 15 June 2016, Accepted 8 September 2016, Scheduled 12 September 2016

* Corresponding author: Andrea Francesco Morabito (andrea.morabito@unirc.it).

[1] DIIES Department, University of Reggio Calabria, Reggio Calabria, Italy. [2] DIEEI Department, University of Catania, Catania, Italy. [3] CNIT (Consorzio Nazionale Interuniversitario per le Telecomunicazioni), Viale G. P. Usberti n. 181/A, I-43124 Parma, Italy.

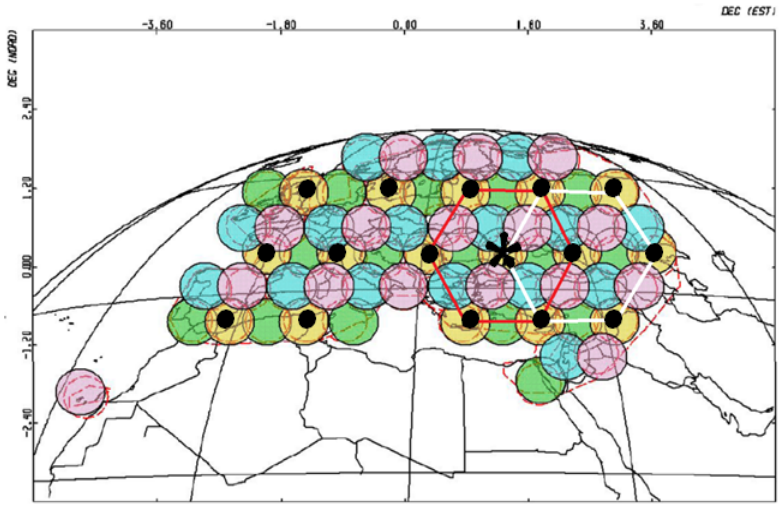

Figure 1. Multibeam coverage of the Europe from GEO satellite (courtesy of Space Engineering S.p.A.). Basically, the mission aims at maximizing the antenna directivity inside the spot marked with * subject to sidelobe upper bounds inside the spots marked with • [8–11].

Once such a mission scenario is defined, the problem can be formulated as that of synthesizing an antenna able to maximize the minimum guaranteed directivity inside the coverage zone while ensuring an adequate Carrier-to-Interference ratio (C/I) or Sidelobe Level (SLL) performance in each beam [4, 8–11]. Whatever the choice of the final antenna, the identification of a continuous aperture source [8] fulfilling 'at best' the required specifications allows to a-priori ascertain the ultimate achievable radiation performance and represents also a 'reference solution' for the optimal synthesis of sparse [9], thinned [10], and clustered [11] Direct Radiating Arrays (DRA).

Notably, the state-of-the-art approaches proposed to realize the map shown in Fig. 1 involve *circularly-symmetric* field distributions, as they are the most attractive choice to perform the consequent design of isophoric DRA [8–11]. For instance, the approach in [8] provides a Convex Programming (CP) procedure for the synthesis of continuous aperture sources realizing a circularly-symmetric directivity pattern fulfilling the requirements represented in Fig. 1. However, by observing Fig. 1 it can be readily noted that, for each beam, the nearest 'iso-color' regions (i.e., the nearest interfering spots) are located over *only six* spatial directions. As a consequence, for a fixed elevation angle, the imposition of the C/I or SLL mission constraints over *all* the azimuthal radiation directions goes well beyond the specifications actually sufficient to realize the coverage. In particular, by fulfilling the C/I or SLL constraints not only on the 'iso-color' regions but also on the non-interfering spots, circularly-symmetric sources (and fields) unnecessarily over constrain the optimization problem.

In the light of the above considerations, it is clear that the ideal solution of the above coverage problem is given by sources showing an *hexagonally-symmetric* behavior in terms of the azimuth angle, which constitute the subject of the design approach proposed in this paper. In fact, such a kind of sources will allow enforcing upper-bound constraints on the sidelobes *only* where it is actually needed, i.e., just on the interfering spots. Therefore, these solutions, opposite to the state-of-the-art ones, will lead to the best exploitation of the antenna-synthesis degrees of freedom and hence to the achievement of the maximum feasible performance in terms of C/I and SLL.

In the following, we propose a new approach to the synthesis of continuous aperture sources such to realize the four-colors multibeam coverage while maximizing the antenna directivity and guaranteeing a fixed isolation between the central beam and the interfering beams. In particular, in Section 2 a field representation optimally suited 'by its nature' to the four-colors map scenario (and easily exploitable to realize any kind of field azimuthal symmetry) is introduced, and in Section 3 the overall synthesis is reduced to a CP problem. Then, in Section 4 the devised approach is tested against requirements and goals recently set by ESA for the multibeam coverage of the Europe from GEO satellites. Conclusions follow.

2. IDENTIFYING THE OPTIMAL REPRESENTATION OF THE FIELD

In order to come to an effective formulation of the problem at hand, some convenient representation is required for the electromagnetic source. Obviously, besides avoiding 'superdirective' solutions [12], such representation should be able to describe the largest set of sources reflecting all the required symmetry properties. Moreover, in order to simplify the optimization procedure by virtue of the reduced number of unknowns, it should be *compact* [13–15]. Finally, as the achieved sources will serve as a reference and as a guide in the synthesis of actual radiating systems, the representation should guarantee some control on the physical features of the source (including its spatial variability and dynamic range). Finally, concerning the geometrical and spectral properties of the aperture and far fields' distributions, the representation should guarantee that:

- the far field and the corresponding power pattern are *bandlimited* functions (the latter having a bandwidth double with respect to that of the former);
- the source must have a circular support of radius a (as requested by usual satellite specifications [8–11]);
- the square-amplitude far-field distribution must exhibit a hexagonal symmetry with respect to the observation azimuth angle (in such a way to perfectly match the map depicted in Fig. 1).

For all the above, an optimal representation simultaneously fulfilling all these requirements consists in expanding the field as a superposition of basis functions similar to the $\mathrm{TE}_{6n,m}$ propagation modes (wherein n and m are non-negative integers) [16] of a circular waveguide of radius a. In fact, in addition to the satisfaction of all the above specifications, these modes allow one to exclude point-wise representations and provide both a closed-form expression for the far field and some control of radial variations of the pattern along the aperture.

Therefore, by denoting ρ and φ as the radial and azimuthal coordinates in the aperture plane, respectively, the sought aperture field E_{AP}, defined over a circular domain of radius a, has been expanded in the set of the unknowns complex coefficients $\{A\}$ as:

$$E_{AP}(\rho,\varphi) = \sum_{n=0}^{N} \left\{ \sum_{m=1}^{M_n} \left[A_m f_{n,m}(\rho,\varphi) + A_{m+M_n} g_{n,m}(\rho,\varphi) \right] \right\} \tag{1a}$$

wherein, by exploiting the guidelines of [16], the f and g basis functions have been chosen as:

$$f_{n,m}(\rho,\varphi) = \cos(6n\varphi)\, J_{6n}\left(\Phi_{6n,m}\frac{\rho}{a}\right) \tag{1b}$$

$$g_{n,m}(\rho,\varphi) = \sin(6n\varphi)\, J_{6n}\left(\Phi_{6n,m}\frac{\rho}{a}\right) \tag{1c}$$

being J_n the Bessel function of first kind and order n, $\Phi_{n,m}$ the m-th root of the first derivative of J_n, $N+1$ the overall number of radiating modes adopted in the expansion, and $2M_n$ the number of unknown coefficients for the $\mathrm{TE}_{6n,m}$ mode. Beside guaranteeing the desired field's symmetry, thanks to their orthogonality in the space of the square integrable functions, such basis functions allow a simple computation of the power flowing through the antenna aperture.

By exploiting the formula in [17], it can be easily shown that the two-dimensional Fourier Transform of $E_{AP}(\rho, \varphi)$, which represents (apart from inessential constants) the far field radiated by the sought source [8], results equal to:

$$E(\theta,\phi) = 2\pi \sum_{n=0}^{N} (-1)^n \left\{ \sum_{m=1}^{M_n} \left[A_m \cos(6n\phi) + A_{m+M_n} \sin(6n\phi) \right] F_{6n,m}(\theta) \right\} \tag{2a}$$

with

$$F_{6n,m}(\theta) = \frac{\Phi_{6n,m} J_{6n}(\beta a \sin\theta) J_{6n-1}(\Phi_{6n,m}) - \beta a \sin\theta J_{6n-1}(\beta a \sin\theta) J_{6n}(\Phi_{6n,m})}{(\beta\sin\theta)^2 - \left(\frac{\Phi_{6n,m}}{a}\right)^2} \tag{2b}$$

where θ and ϕ denote the elevation and azimuth angles spanning the observation space, respectively, and $\beta = 2\pi/\lambda$ (λ denoting the wavelength) is the wavenumber.

It is interesting to note that the reasonings made above about the choice of basis functions in Eqs. (1b) and (1c) are quite general and could be exploited to identify field expansions exhibiting any desired symmetry with respect to the aperture azimuth angle.

Notably, before exploiting the above field representation the user has to perform an optimal choice of the N and M_n values, which can allow not only avoiding the occurrence of superdirective sources but also guaranteeing a smooth amplitude distribution to the synthesized aperture fields (which is in turn essential to effectively perform their discretization into DRA [9–11]). A first guide to optimally perform such a choice is provided by the observation of the singular values [15] of 'radiation' operator relating (1a) and (2a). Alternative simple ways for properly truncating the above expansions can be identified thorough the following simple reasonings.

Concerning the M_n value, for any fixed index n it allows to control the number of *radial* oscillations of the field [16]. In particular, larger M_n values provide the capability of fulfilling harder SLL and beamwidth constraints over the radial coordinate of the spectral plane. On the other hand, in order to avoid superdirective sources [12], M_n must be chosen according to the rules defined in [13, 14], i.e., it should not exceed the *number of degrees of freedom* of the field associated to $\mathrm{TE}_{6n,m}$ mode. Hence, M_0 should not be larger than $2a/\lambda$, which has been defined in [13] as the critical value of the bandwidth of a circularly-symmetric source of radius a. For $n \neq 0$, any increase of $|n|$ entails a relevant increase of the number of zeroes (and oscillations) of the J_{6n} functions appearing inside (1b), (1c), (2b). Therefore, the larger n, the lower the optimal value of M_n results.

Concerning N, such a parameter corresponds to the number of modes exploited (in addition to the $\mathrm{TE}_{0,m}$) to compose the overall radiated field. Therefore, for any fixed M_n, the N value allows to control the number of the *azimuth* oscillations of the field [16]. In particular, larger N values will provide a better 'interlocking' of the synthesized field inside the coverage map (see Fig. 1), i.e., a better capability of optimizing the SLL or C/I performances exactly over the interfering spots. On the other side, for $n \neq 0$ all $J_n(x)$ functions exhibit for $x = 0$ a null having a width proportional to n. Therefore, by virtue of the J_{6n} functions appearing inside Eqs. (1b), (1c), (2b), an arbitrarily large value of N could produce poor power-pattern performances in center of the spectral plane.

Finally, the overall number of field contributions constituting Eq. (2a) should not exceed the overall number of *degrees of freedom* of the source, i.e., N and M_n should obey the following rule:

$$2\sum_{n=0}^{N} M_n \leq \frac{\textit{area of the source}}{(\lambda/2)^2} = 4\pi\left(\frac{a}{\lambda}\right)^2 \tag{3}$$

In the following, the presented field representation is exploited to devise an effective source synthesis procedure.

3. THE SYNTHESIS PROCEDURE

In the following we present the synthesis approach with reference to a source pointing at boresight. This does not induce any loss of generality, as the beam can be conveniently steered to any desired direction by means of a proper linear phase shift and scanning losses can be tackled by strengthening the requirements on the far-field.

By using expansions in Eqs. (1), (2), the problem of the synthesis of a continuous aperture source realizing at best the four-color multibeam coverage depicted in Fig. 1 has been formulated as follows:

Determine the set of coefficients $\{A\}$ *such that:*

$$\int_0^{2\pi}\int_0^{\frac{\pi}{2}} |E(\theta,\phi)|^2 \sin\theta d\theta d\phi \quad \textit{is minimized} \tag{4a}$$

subject to:

$$\mathrm{Re}\left\{E(\theta_{\mathrm{EOC}},\phi^*)\right\} \geq 1 \tag{4b}$$

$$|E(\theta,\phi)|^2 \leq UB(\theta,\phi) \quad \textit{in the interfering spots} \tag{4c}$$

wherein θ_{EOC} denotes the Edge of Coverage (EOC) [8–11] elevation angle, i.e., the border of the central spot (which is marked with '*' in Fig. 1), while φ^* is an arbitrary value of φ, and UB is a real and non-negative function allowing the fulfilment of the SLL constraints.

Let us now discuss the physical meaning of optimization problem in Eq. (4). As long as the central spot is sufficiently narrow (which is indeed true in any multispot Earth coverage realized form GEO satellites), the joint consideration of constraints in Eqs. (4b), (4c) provides the desired isolation amongst 'iso-color' beams, while the joint consideration of Eqs. (4a), (4b) allows to maximize the directivity within the central spot [8]. The reasons underlying such statements are given in the following.

Let us first consider the meaning of constraint in Eq. (4b). Without any loss of generality, the arbitrary reference phase can be fixed in such a way that the field is real in the specific directions $(\theta_{\mathrm{EOC}}, \varphi^*)$ [18], which allows to deal with a linear constraint in terms of the real and imaginary parts of the unknown coefficients $\{A\}$. As long as the observation angle is sufficiently small, only the terms having $n = 0$ have to be considered in expression (2). In fact, since $J_n(0) = 0$ for any $|n| \neq 0$, the higher order terms will be negligible and the only 'excited' mode will be the $\mathrm{TE}_{0,m}$, leading within the central spot to a (nearly) circularly-symmetric field. Under such circumstances, constraint in Eq. (4b) guarantees that the field is greater than or equal to 1 along the entire boundary of the spot. Moreover, if $\sin(\theta_{EOC})$ is smaller than the *Nyquist Distance* $\pi/\beta a$, i.e., than the minimum distance between two independent samples of the radiated field [13], then the fulfilment of constraint in Eq. (4b) along the boundary of the spot implies that the field amplitude will be greater than the one in the whole spot (i.e., for each $\theta \in [0, \theta_{\mathrm{EOC}}]$) [8]. Therefore, the contemporaneous enforcement of both constraints in Eqs. (4b) and (4c), and a proper choice of the 'upper bound' mask UB, will ensure that the central beam pattern will be sufficiently small in the 'iso-color' regions, thus providing the desired isolation amongst the interfering beams.

To get a better understanding of the characteristics of the UB function, a pictorial view of the mask required to realize the coverage of Fig. 1 (and used to generate the results shown in Section 4) is shown in Fig. 2. In the latter, the green circle represents the boundary of the central spot, i.e., the EOC perimeter, while the red regions correspond to 'iso-color' spots wherein the central beam's pattern has to be lower than a fixed threshold depending on desired performance in terms of C/I. As discussed in [18], constraints in Eq. (4c) are convex in terms of the unknowns $\{A\}$.

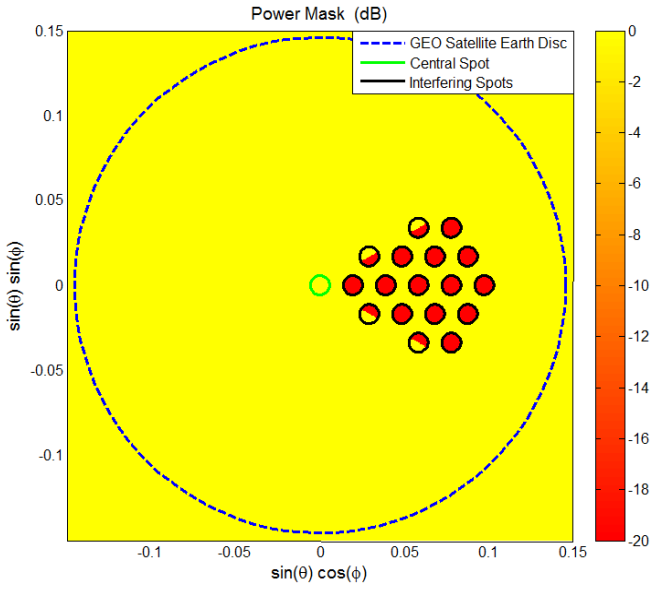

Figure 2. Power-pattern mask adopted to shape the directivity in such a way to realize the coverage shown in Fig. 1. Notably, in imposing the constraints it is sufficient, by virtue of the nature of the adopted electromagnetic field's basis functions, to span just a $\pi/3$ azimuthal range of the observation domain.

Let us consider now the cost function in Eq. (4a). It is quadratic and positive semi-definite in terms of the unknowns and represents the *radiated power*. Its minimization implies that the power pattern will be as small as possible within the mask enforced by Eqs. (4b) and (4c), so that the field at the boundary of the central spot, i.e., the field in Eq. (4b), will be exactly equal to 1 for $\theta = \theta_{EOC}$. Under such conditions, Eq. (4b) can be seen as an *equality* (convex) constraint. Then, by definition of directivity, minimizing the radiated power subject to an equality constraint on the field at the EOC angle means to maximize the directivity attained for $\theta = \theta_{\rm EOC}$ [8].

For all the above, it is possible to state that the problem in Eq. (4):

(i) enforces the maximization of the EOC directivity (and within the whole central spot) while guaranteeing the desired 'power separation' amongst the central spot and the 'iso-color' regions;

(ii) is a CP one and hence, provided that an intersection amongst the listed constraints does exist, it guarantees the fast achievement of the unique and globally optimal solution.

In the following, the actual capabilities of the approach are tested in a realistic synthesis scenario characterized by extremely hard antenna requirements.

4. AN ASSESSMENT OF PERFORMANCES IN A REALISTIC SCENARIO

In order to evaluate the actual effectiveness and usefulness of the proposed approach, its performance have been tested against the realistic scenario set by ESA (see [8–11]). The ultimate performances achievable by a circularly-symmetric continuous source in this scenario have been determined in [8], and the aim of what follows includes the identification of 'whether and up to what extent' they can be improved by means of the proposed approach.

Coming to details, the ESA Invitations to Tenders (ITT) recalled in [8–11] requires the realization of spots having a diameter of 0.65° (i.e., $\theta_{\rm EOC} = 0.325°$) and located with a center-to-center constant spacing of 1.12°. The source must cover a circular aperture having a radius not larger than 60λ and realize an EOC directivity not lower than 43.8 dBi. Finally, the maximum directivity inside each 'iso-color' spots must be at least 20 dB lower than the EOC directivity. All requirements are rigorously taken into account by the power mask depicted in Fig. 2, wherein the green circle represents the boundary of the central spot while the red regions correspond to 'iso-color' spots.

In the following two subsections, the outcomes of two separate 'optimal synthesis' [19] numerical experiments are respectively presented: first, we identified the maximum SLL performance for a fixed size of the source; second, we determined the minimum feasible size of the source able to guarantee the lowest acceptable SLL performance. The results achieved in the two test cases are summarized in Table 1, wherein they are also compared with the requirements of the ESA mission scenario and the performances obtained in [8]. In both cases, in order to fulfil the criteria listed in Section 2 and to assign the same 'weight' to each field mode, we chose $N = 3$ and $M_0 = M_1 = M_2 = M_3 = 10$.

Table 1. Summary of the technical specifications for the ESA multibeam coverage of the Europe from GEO satellites and comparison between the achieved performances and the results in [8].

	Source radius	**EOC Directivity**	**Maximum SLL with respect to EOC**
[4] (European Space Agency goals)	$\leq 60\lambda$	≥ 43.8 dBi	≤ -20.0 dB
[8] (Circularly-symmetric fields)	60 λ	46.8 dBi	-22.2 dB
[8] (Circularly-symmetric fields)	50 λ	46.6 dBi	-20.0 dB
Results in Section 4.1	50 λ	46.3 dBi	-25.6 dB
Results in Section 4.2	43 λ	45.5 dBi	-20.5 dB

4.1. Maximizing the Radiation Performance for a Fixed Size of the Source

In the first example, a source having a radius equal to 50λ has been considered, and problem (4) has been iteratively solved by requiring lower and lower power-pattern values in the red regions of the *UB* mask (see Fig. 2) until constraints became so strict to prevent the existence of a solution. The achieved results are represented in Figs. 3 and 4. In particular, Fig. 3 shows the synthesized continuous aperture source [sub-plot (a)] and the corresponding directivity [sub-plot (b)], while Fig. 4 provides further detailed views of the radiation performance. In all directivity plots we show also the Earth disc as seen from GEO satellites (consisting in a circle of radius 8.4°), the boundary of the central spot, and a pictorial view of all the interfering spots. As it can be seen, the proposed approach allowed to satisfy all the constraints on the 'iso-color' beams and to achieve a SLL 5.6 dB lower than the one achieved in [8] through a source having the same size (see Table 1). Moreover, the directivity attained at the EOC angle, i.e., 46.3 dBi, results just 0.3 dB lower than the one achieved in [8] through a source of the same size and just 0.5 dB lower than the one achieved in [8] through a source having a 20λ larger diameter.

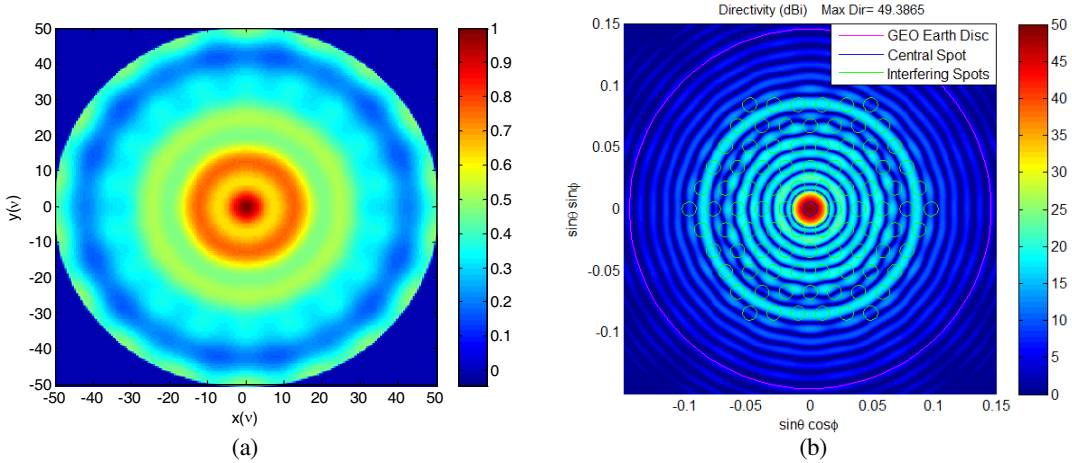

Figure 3. First test case: (a) source synthesized over an aperture of radius 50λ and (b) corresponding directivity plotted in the spectral plane.

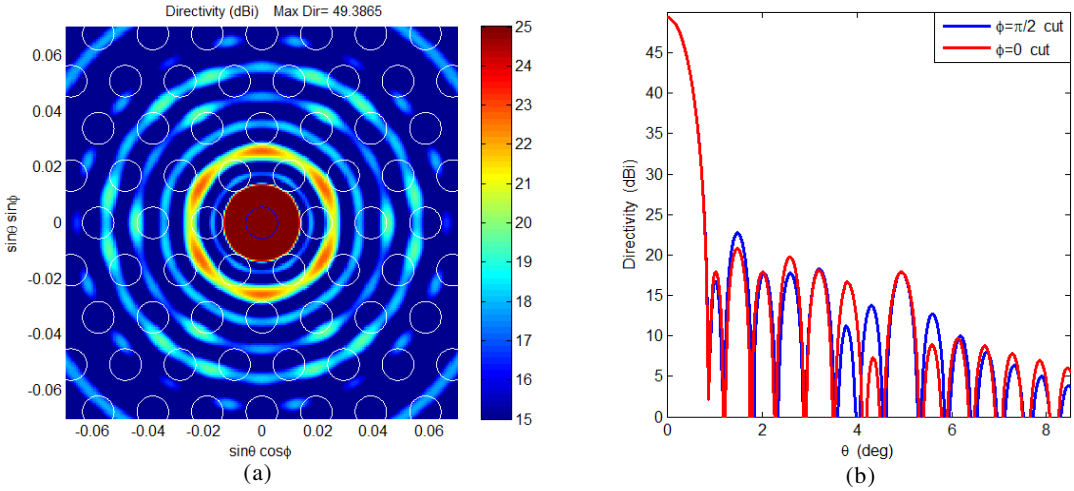

Figure 4. Pictorial views of the directivity shown in Fig. 3: (a) zoom and thresholding to the range 15–25 dBi and (b) main cuts through central beam. White circles in subplot (a) represent the interfering spots: as desired, the radiation creates null fields on the adjacent spots, where the other beams appear, in order to reduce interferences.

The maximum directivity of the synthesized source is 49.4 dBi and hence results just 0.54 dB lower than the theoretical maximum directivity achievable through a source of the same size and computable as:

$$10\log_{10}\left(\frac{4\pi}{\lambda^2}area\ of\ the\ source\right) = 10\log_{10}\left[4\left(\frac{\pi a}{\lambda}\right)^2\right] \tag{5}$$

It can be concluded that the synthesized solutions actually take advantage from variations in both the elevation and azimuth angles, which cannot be the case as long as circularly-symmetric sources are used.

4.2. Identifying the Minimum Feasible Size of the Source

By enforcing (with respect to the EOC power) a SLL lower than -20.5 dB, i.e., 0.5 dB lower than the one adopted in [8], we have solved problem (4) for lower and lower a values until constraints became

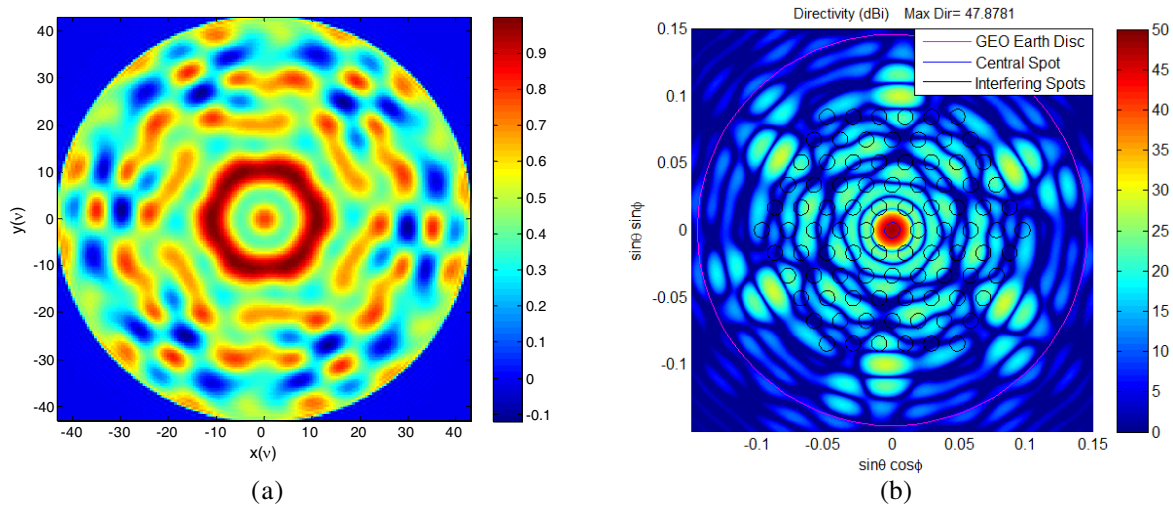

Figure 5. Second test case: (a) source synthesized over an aperture of radius 43λ and (b) corresponding directivity plotted in the spectral plane.

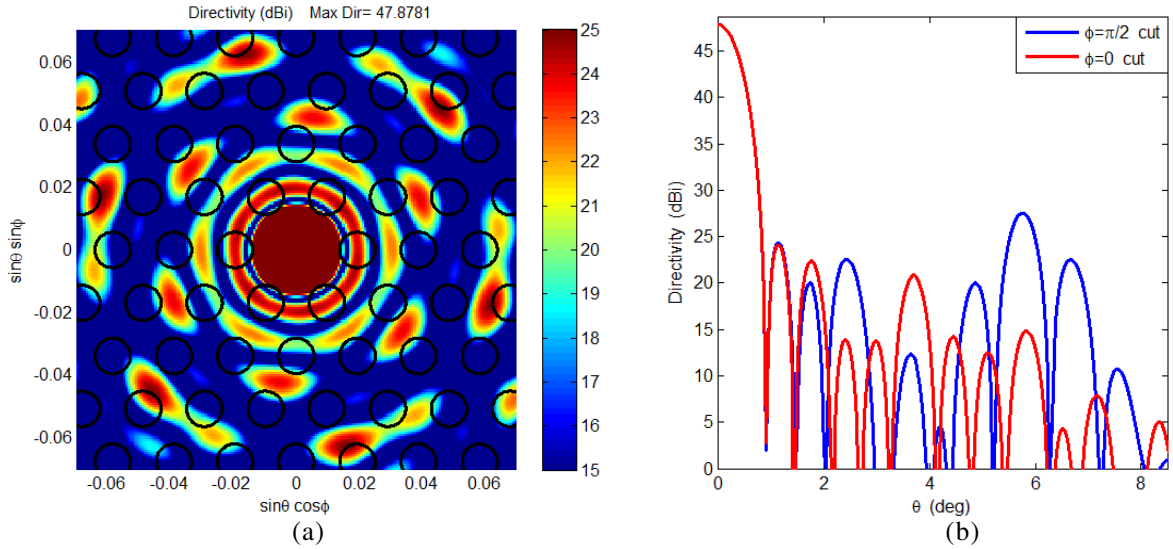

Figure 6. Pictorial views of the directivity shown in Fig. 5: (a) zoom and thresholding to the range 15–25 dBi and (b) main cuts through central beam. Black circles in subplot (a) represent the interfering spots: as required, the radiation results low inside the interfering spots.

so strict to prevent the existence of a solution. By so doing, we identified the minimum radius of a feasible source able to satisfy all the ESA requirements. The outcomes of the proposed procedures are shown in Figs. 5 and 6. In particular, Fig. 5 shows both the achieved aperture-field distribution (which turns out having a radius equal to 43λ) and the corresponding directivity. Similarly to Fig. 4, Fig. 6 provides a convenient zoom of the directivity in the spectral plane and a representation of the main cuts (through the central beam) of the radiation pattern. Both Figs. 5 and 6 show a pictorial view of all the interfering spots. In this case, the directivity achieves a maximum value of 47.9 dBi, i.e., just 0.73 dB lower than the maximum theoretical directivity computable through (5), and attains at the EOC angle the value of 45.5 dBi. Again, as can be seen from Fig. 6, decisive advantage is taken from the induced azimuthal variations in the source's spectrum.

5. CONCLUSIONS

The problem of the optimal synthesis of continuous aperture sources fulfilling at best the 'four-colors' geometrical map usually adopted in multibeam GEO satellite telecommunications has been formulated and solved. Decisive advantage has been taken from the capability of separately controlling the radial and angular field behaviors, which allows a 'smart interlocking' amongst the interfering beams and the highest sidelobes of the central beam. Thanks to the adopted formulation, the radiation creates null fields on the adjacent spots, where the other beams appear, in order to reduce interferences. Such a circumstance allows remarkable performance improvements with respect to the state-of-the-art available solutions.

By following the same guidelines leading from [8] to [9–11, 20, 21], the achieved solutions can be used to design isophoric DRA.

Finally, the approach is very flexible and general as a proper change of the basis functions inside the adopted field's expansion can allow inducing any kind of angular symmetry on the power pattern distribution.

REFERENCES

1. Bailleul, P. K., "A new era in elemental digital beamforming for spaceborne communications phased arrays," *Proceedings of the IEEE*, Vol. 104, No. 3, 623–632, 2016.
2. Bolt, R. J., D. Cavallo, G. Gerini, D. Deurloo, R. Grooters, A. Neto, and G. Toso, "Characterization of a dual-polarized connected-dipole array for Ku-band mobile terminals," *IEEE Transactions on Antennas and Propagation*, Vol. 64, No. 2, 591–598, 2016.
3. Morabito, A. F., T. Isernia, and L. Di Donato, "Optimal synthesis of phase-only reconfigurable linear sparse arrays having uniform-amplitude excitations," *Progress In Electromagnetics Research*, Vol. 124, 405–423, 2012.
4. Fonseca, N. J. G., J.-C. Angevain, and C. Mangenot, "Toward the terabit/s satellite: Antenna design trade-offs and analyses," *Proceedings of the 33rd European Space Agency Antenna Workshop*, 2011.
5. Rao, S. K., "Parametric design and analysis of multiple-beam reflector antennas for satellite communications," *IEEE Antennas and Propagation Magazine*, Vol. 45, No. 4, 26–34, 2003.
6. Fonseca, N. J. G. and J. Sombrin, "Multi-beam reflector antenna system combining beam hopping and size reduction of effectively used spots," *IEEE Antennas and Propagation Magazine*, Vol. 54, No. 2, 88–99, 2012.
7. Appel, K. and W. Haken, "Every planar map is four colourable, Part I: Discharging," *Illinois Journal of Mathematics*, Vol. 21, 429–490, 1977.
8. Bucci, O. M., T. Isernia, and A. F. Morabito, "Optimal synthesis of directivity constrained pencil beams by means of circularly symmetric aperture fields," *IEEE Antennas and Wireless Propagation Letters*, Vol. 8, 1386–1389, 2009.
9. Bucci, O. M., T. Isernia, A. F. Morabito, S. Perna, and D. Pinchera, "Density and element-size tapering for the design of arrays with a reduced number of control points and high efficiency,"

Proceedings of the Fourth European Conference on Antennas and Propagation, EuCAP 2010, Barcelona, Spain, April 12–16, 2010.

10. Bucci, O. M., T. Isernia, and A. F. Morabito, "A deterministic approach to the synthesis of pencil beams through planar thinned arrays," *Progress In Electromagnetics Research*, Vol. 101, 217–230, 2010.
11. Morabito, A. F., T. Isernia, M. G. Labate, M. D'Urso, and O. M. Bucci, "Direct radiating arrays for satellite communications via aperiodic tilings," *Progress In Electromagnetics Research*, Vol. 93, 107–124, 2009.
12. Rhodes, D. R., "On the quality factor of strip and line source antennas and its relationship to superdirectivity ratio," *IEEE Transactions on Antennas and Propagation*, Vol. 20, No. 3, 318–325, 1972.
13. Bucci, O. M., C. Gennarelli, and C. Savarese, "Representation of electromagnetic fields over arbitrary surfaces by a finite and nonredundant number of samples," *IEEE Transactions on Antennas and Propagation*, Vol. 46, No. 3, 351–359, 1998.
14. Bucci, O. M. and G. Franceschetti, "On the degrees of freedom of scattered fields," *IEEE Transactions on Antennas and Propagation*, Vol. 37, No. 7, 918–926, 1989.
15. Bertero, M. and P. Boccacci, "Singular value decomposition," *Introduction to Inverse Problems in Imaging*, 1st Edition, Section 9, 220–246, CRC Press, 1998.
16. Collin, R. E., "Circular waveguides," *Foundations of Microwave Engineering*, 2nd Edition, 194–198, IEEE Press, Wiley Interscience, New York, 1992.
17. Gradshteyn, I. S. and I. M. Ryzhik, *Table of Integrals, Series and Products*, 6th Edition, 653–662, Academic Press, USA, 2000.
18. Isernia, T. and G. Panariello, "Optimal focusing of scalar fields subject to arbitrary upper bounds," *Electronics Letters*, Vol. 34, No. 2, 162–164, 1998.
19. Bucci, O. M., T. Isernia, and A. F. Morabito, "Optimal synthesis of circularly symmetric shaped beams," *IEEE Transactions on Antennas and Propagation*, Vol. 62, No. 4, 1954–1964, 2014.
20. Viganó, M. C., G. Toso, G. Caille, C. Mangenot, and I. E. Lager, "Sunflower array antenna with adjustable density taper," *International Journal of Antennas and Propagation*, Vol. 2009, 10 pages, Article ID 624035, doi:10.1155/2009/624035, 2009.
21. Angeletti, P., G. Toso, and G. Ruggerini, "Array antennas with jointly optimized elements positions and dimensions, Part II: Planar circular arrays," *IEEE Transactions on Antennas and Propagation*, Vol. 62, No. 4, 1627–1639, 2013.